JOURNAL OF MATERIALS SCIENCE 33 (1998) 2529–2535

Influence of weathering on unreinforced and short glass fibre reinforced thermoplastic polyester

N. S. CHOI*, K. TAKAHASHI‡
Research Institute for Applied Mechanics, Kyushu University, Kasuga-shi, Fukuoka 816 Japan

D. OSCHMANN, J. KARGER-KOCSIS, K. FRIEDRICH
Institut für Verbundwerkstoffe GmbH, University of Kaiserslautern, D-67663 Kaiserslautern, Germany
E-mail: ktakaha@riam.kyushu-u.ac.jp

The influence of weathering on fracture toughness, J_c, yield strength, σ_y, local ultrasonic velocity, V_R, and microhardness, H_u, in unreinforced and a short glass-fibre-reinforced polyester-based thermoplastic "Xenoy" has been investigated. Unreinforced material weathered for 11 months outdoors in Perth, West Australia, exhibited a significant decrease in V_R and J_c, whereas little change was shown in σ_y, H_u and the fracture surface morphology. Irradiation for 1000 h by artificial ultraviolet rays upon the unreinforced material caused a considerable increase in H_u and only a slight deterioration in V_R of the surface layer. Filling with the short fibres induced an improvement in σ_y and a large reduction in J_c for the unreinforced material. The natural weathering of the reinforced material caused a small reduction in J_c but a large degradation in the slope of the *R*-curve. It was concluded that the measurement of J_c and the slope of *R*-curve in combination with V_R and H_u was an effective way to study the effects of weathering on engineering plastics.

1. Introduction

Polymer-matrix composites have been extensively applied to various structural components, such as sporting goods, automobiles, yacht and aerospace vehicles, due to their high specific stiffness and strength. However, polymers are liable to degrade when they are subjected to natural weathering conditions such as sunlight, moisture and rain.

Qayyum and White [1] studied the effect of weathering on injection-moulded polymers and showed that the tensile residual stresses near the surface tended to become greater, which caused surface damage easily and a change in the failure mechanism. Thermal ageing effects on impact fracture energy and phase separation of a blend consisting of amorphous polycarbonate (PC) and crystalline PBT were studied by Bertilsson *et al.* [2, 3]. Applying various loading modes for polypropylene (PP) and polyamide 6 (PA6) after natural and artificial weathering, Just [4] reported morphological changes on the weathered surface and claimed that flexural impact strength and strain at break reflect the weathering most sensitively. Emphasizing the significance of the wavelength of the incident light, Sommer and co-workers [5, 6] investigated the primary process of photodegradation in polymers under artificial weathering and suggested a method for accelerated weathering. Sebaa *et al.* [7] studied the weathering behaviour of low-density polyethylene films by a calorimetric analysis. Using Fourier transform–infrared transmission microscopy, Campeotto *et al.* [8] investigated weathering of thermoplastic blends of PA6.6/polyphenylene oxide (PPO) and PC/PBT and suggested ultraviolet-ray oxidative degradation and photolytic chain scission of the polyblends. Molecular weight decrease in the weathered thermoplastics was reported by Shiroda [9]. Czigány *et al.* [10] reported hydrolysis degradation and fracture toughness decrease of short glass-fibre-reinforced, toughened poly(butylene terephthalate) (PBT).

In this paper, the effects of weathering on unreinforced and short glass-fibre-reinforced PC/PBT thermoplastic blend "Xenoy" were studied. Measurements of global-scale properties, such as yield strength and fracture toughness of the materials, were performed in combination with local-scale measurements of ultrasonic velocity and microhardness, to investigate the effects.

2. Experimental procedure

2.1. Materials

As described above, unreinforced and short glass-fibre (SGF)-reinforced Xenoy thermoplastics were tested in

**Present address*: Department of Mechanical Engineering, Hanyang University, Ansan-shi 425-791, Korea.
‡Author to whom all correspondence should be addressed.

this study. Unreinforced Xenoy (Xenoy 5220u produced by General Electric Plastics Co.) was a thermoplastic blend of PC/PBT. The fibre weight fraction of the composite was 31%. Injection-moulded plates, 2.75 mm thick, were exposed to the following weathering conditions: (1) unweathered; (2) naturally weathered for 11 months outdoors in Perth, West Australia, under the conditions which follow the Australian standard A1580-457.1. According to the standard, test panels should be shadow-free, placed higher than 60 cm from the ground, face north and inclined at an angle of 45° to the vertical plane; (3) artificially weathered indoors for 1000 h, during which the irradiation was performed vertical to the plate surface at 60 °C by ultraviolet rays (UVRs) with a 313 nm principal wavelength.

Compact tension (CT) specimens of 35 mm long and 35 mm wide were machined from the plate. As shown in Fig. 1, the specimens were notched perpendicular (T direction) and parallel (L direction) to the mould-fill direction using a diamond wheel cutter with a thickness of 0.4 mm. A sharp notch was introduced by pushing a razor blade into the initial notch tip. The initial crack length, a_0, was kept to 17.0 ± 0.2 mm. Dumb-bell type tensile specimens were also obtained in the directions of T and L, as shown in Fig. 1. In addition, microhardness and ultrasonic test specimens were machined from the central part of the plates.

2.2. Tensile testing and *J*-integral evaluation

Tensile testing was performed at a crosshead speed of 0.5 mm min^{-1} using dumb-bell type and compact tension type specimens. Five specimens were tested for each experimental condition. The maximum stress obtained from the measured nominal stress–strain curve was taken as a value corresponding to the yield strength, σ_y [11]. Based on the Landes and Begley method [12, 13] which employed several specimens, values of the *J*-integral were evaluated as a function of crack propagation length, Δa, by the following equation

$$J = \frac{\eta_p^* U_T}{B b} \quad (1)$$

where U_T is the deformation energy obtained from the load, *P*, – displacement, δ curves of CT specimens, *B* the specimen thickness, *b* the ligament length, η_p^* the Merble and Corten's compensation coefficient [13] for the plastic region ahead of the crack tip, the value of which varies with a/b and is 2.27 at $a/b = 1$. The value of Δa was obtained as an average of eight values for the crack in order to consider the eventual curved form of the crack tip front. A number of identically cracked specimens were loaded up to various displacements producing different amounts of crack extension, Δa, and then unloaded. For determination of values of *J*, slow fracture surfaces of the tested specimens were examined after impact fracture under a cryogenic condition. Values of fracture toughness, J_c, were measured at the joining point between the blunting line given from equation

$$J = 2\sigma_y \Delta a \quad (2)$$

and the crack resistance, *R*, curve determined from Equation 1. Values of σ_y for the CT specimens notched in the T and L directions were obtained from averaged values of σ_y for dumb-bell type tensile specimens in the L and T directions, respectively (see Fig. 1).

2.3. Fracture surface observation

Fracture surfaces of CT specimens were observed under a scanning electron microscope (SEM) to study weathering effects on the fracture behaviour.

2.4. Local ultrasonic velocity measurement

Ultrasonic velocity was measured at a location on a polished cross-section of the plate employing a scanning acoustic microscope (HSAM 200, Hitachi Co.) as shown in Fig. 2. Longitudinal plane waves with a frequency of 400 MHz travelled through the distilled water and were point-focused on the surface layer of

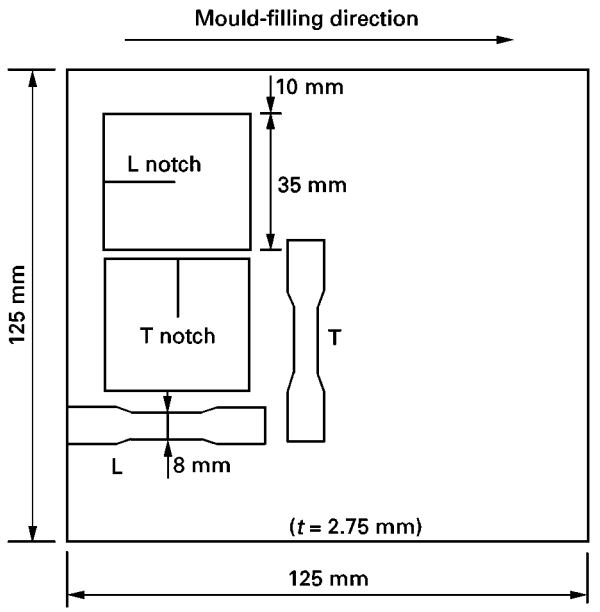

Figure 1 Geometry of the injection-moulded plate and the compact tension (CT) and dumb-bell type specimens.

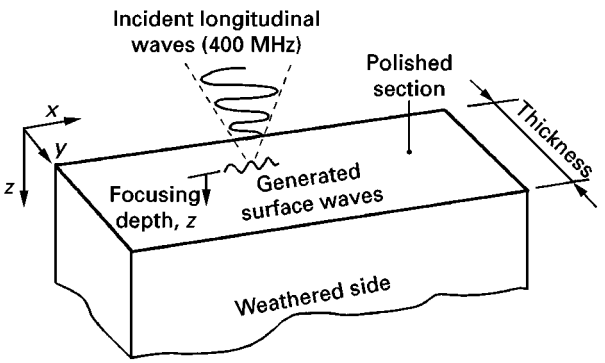

Figure 2 Measurement of the velocity, V_R, of elastic surface waves propagating locally in the surface layer using an acoustic microscope.

the cross-section by an acoustic lens. By analysing the variation in the amplitudes of the reflected waves with different focusing depth (z direction) from the surface, the velocity of the elastic surface waves, V_R, propagating through the surface layer of 10–30 μm depth, was measured using the equation [14]

$$V_R = (V_0 f \Delta z)^{1/2} \quad (3)$$

where V_0 is the longitudinal wave velocity of the water coupler; f the frequency of the longitudinal waves; Δz the average distance between focusing depths corresponding to the two continual peak amplitudes of the reflected waves. Weathering effects on local ultrasonic velocity were studied in the thickness (y) direction.

2.5. Microhardness measurement

Using a dynamic microhardness tester (DUH-50, Shimadzu Co.), the relative microhardness, H_u, of the polished surface of the unreinforced specimen was measured. The measurement was performed to obtain a value of indentation depth with a method of pushing a diamond triangular indentor perpendicular to the specimen surface under the condition of an initial loading rate 1.9×10^{-3} N s^{-1}, maximum load 0.19 N and load retention time of 20 s. Weathering effects on microhardness were investigated in the thickness direction after the specimen surface was ground and then polished. The microhardness testing was carried out five times for each experimental condition.

3. Results and discussion

3.1. Effect of weathering on yield strength

Results of yield strength, σ_y, measured from dumbbell type tensile specimens are listed in Table I. The reinforcement with 31 wt % fibres in unweathered Xenoy resulted in an increase of σ_y by 43% for L and 32% for T-specimens, respectively. The reinforced specimens showed that σ_y for L-specimens was much higher than that for T-specimens. The larger strength for L-specimens is quite reasonable if we consider that fibres aligned in the L-direction cause high reinforcing efficiency in L-specimens [15, 16]. In the case of unreinforced specimens, larger σ_y values were also obtained for T specimens; this is understandable in view of the fact that the microstructural anisotropy is formed during injection moulding of the plaques [15, 17–19].

TABLE I Weathering effects on the yield strength, σ_y, of unreinforced and SGF-reinforced Xenoy specimens

Materials	Loading direction	σ_y (MPa)	
		Unweathered	Weathered for 11 months
Unreinforced Xenoy	L	$47.8^{+1.9}_{-1.7}$	$48.9^{+1.6}_{-3.1}$
	T	$44.3^{+1.6}_{-1.7}$	$44.7^{+2.0}_{-2.0}$
SGF31 wt % Xenoy	L	$68.7^{+3.8}_{-2.3}$	$68.0^{+2.5}_{-2.9}$
	T	$58.2^{+1.7}_{-0.8}$	$60.4^{+0.9}_{-0.7}$

Values of σ_y for unreinforced and SGF-reinforced specimens were hardly changed by weathering for 11 months. A reduction in ductility of unreinforced Xenoy and a gradual increase in σ_y of glass-fibre-reinforced Xenoy with increasing UVR exposure time were reported in the literature by Campeotto *et al.* [8]. Qayyum and White [1] reported that σ_y of polypropylene (PP) and polyacetal (POM) scarcely changed on weathering for 3 y, whereas nylon (PA6.6) exhibited a 30% decrease in σ_y on being weathered for an initial period of 1.5 y and, after that, σ_y approached a constant value. Fracture strain was lessened largely for those plastics in the order PA 6.6 > POM > PP. The severe deterioration of PA 6.6 was considered mainly due to the influence of humidity in air. The present study revealed that weathering for a period of 11 months rarely affected σ_y of the thermoplastic blend Xenoy.

3.2. Effect of weathering on the fracture toughness and *R*-curve

Fig. 3 shows effects of weathering on load, P, – crack opening displacement, δ curves of unreinforced and SGF31 wt % reinforced specimens notched in the L direction. As compared with unweathered specimens, unreinforced Xenoy weathered for 11 months exhibited a very slight increase in the maximum load. In contrast, reinforced Xenoy showed a considerable loss in ductility, together with some slight decrease in the maximum load.

Fig. 4a presents *R*-curves for unreinforced specimens with L notches. The material weathered for 11 months shortly exhibited lower J-integral values by about 5.4 kJ m^{-2} and a similar slope of the *R*-curve, $dJ/d(\Delta a)$, throughout the whole range of Δa, as compared with the unweathered one. Unreinforced specimens with T notches also showed a feature of reduction in J-integral similar to the above, by the weathering (see Fig. 4b). This consistency in reduction of J-integral for each crack propagation length may indicate that the weathering affected the deterioration of unreinforced Xenoy.

R-curves obtained for SGF-reinforced specimens with L notches are shown in Fig. 5a. Weathering for 11 months induced considerable degradation of the

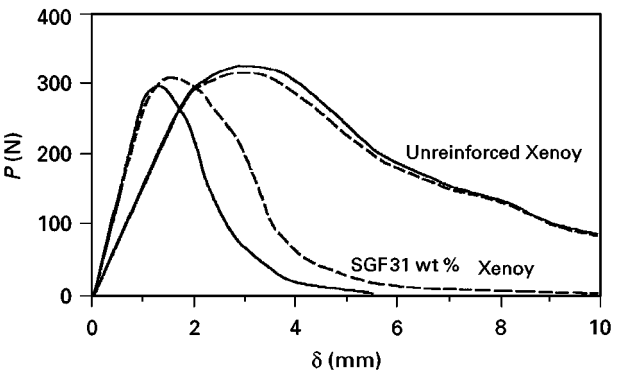

Figure 3 Typical load–displacement curves of unreinforced and SGF-reinforced Xenoy CT specimens with L notches (– – –) unweathered, (—) weathered for 11 months.

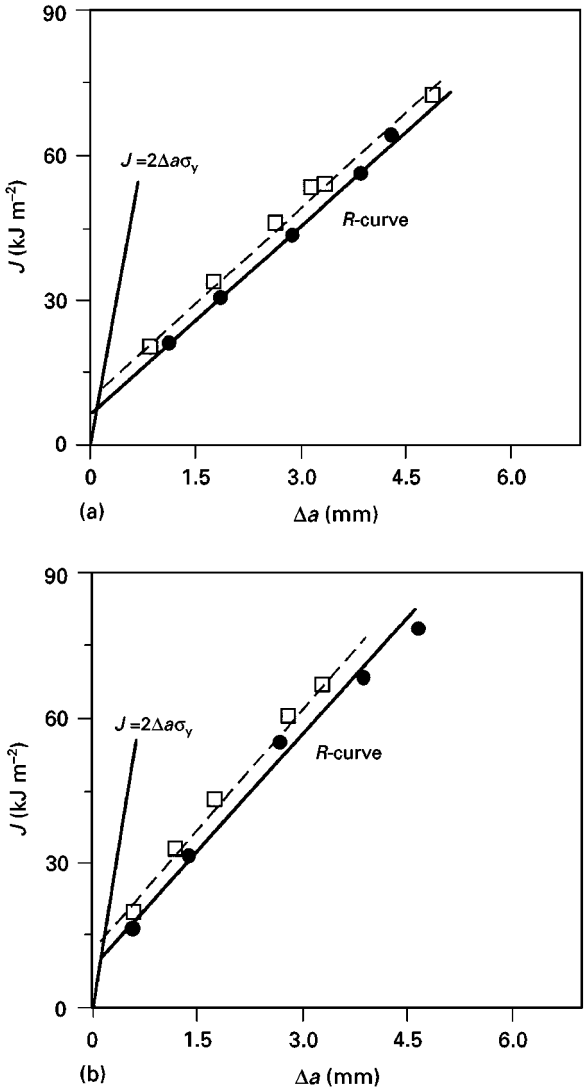

Figure 4 J-integral as a function of crack propagation length, Δa, for unreinforced Xenoy (□) unweathered and (●) weathered for 11 months: (a) L-notched and (b) T-notched specimens.

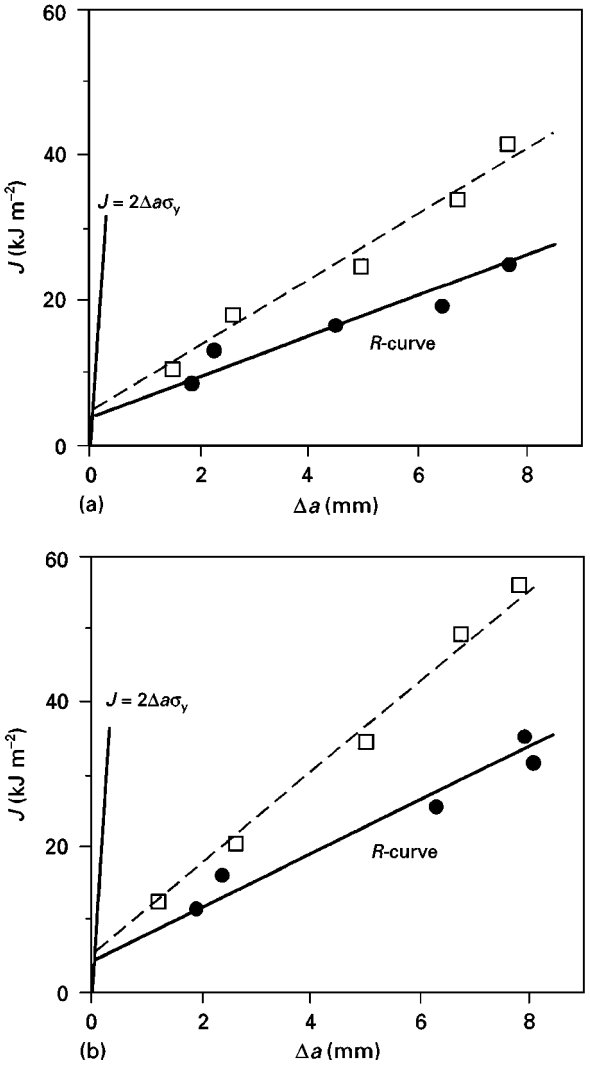

Figure 5 J-integral as a function of crack propagation length, Δa, for the SGF-reinforced Xenoy, (□) unweathered and (●) weathered for 11 months: (a) L-notched and (b) T-notched specimens.

reinforced material: the value of $dJ/d(\Delta a)$ for the weathered material was significantly lower than that for the unweathered material; the amount of reduction in J-integral was about 2.9 kJ m^{-2} at $\Delta a \simeq 2.0$ mm, but the value was much larger (15.2 kJ m^{-2}) at $\Delta a \simeq 7.5$ mm. The R-curve of weathered T notched specimens had features similar to the above (see Fig. 5b).

It should be noted that SGF-reinforced specimens revealed greater degradation in the value of $dJ/d(\Delta a)$ in comparison with unreinforced ones. Considering that the slope of the R-curve indicates the tearing resistance to stable crack growth [13], it is believed that the tearing resistance of SGF-reinforced specimens was deteriorated by weathering. This may be the result of some degradation of the Xenoy matrix and the interface between the matrix and glass fibres. The unreinforced specimens experienced a simple degradation mechanism characteristic for Xenoy.

Values of J_c for each kind of specimen are listed in Table II. The filling of SGF31 wt % caused a large reduction in J_c, i.e. by 60–71%. Unreinforced and SGF-reinforced specimens with T notches exhibited higher J_c values than the corresponding specimens with L notches. After being weathered for 11 months, unreinforced specimens with T notches exhibited the greatest degradation in J_c by about 33%, whereas J_c of SGF-reinforced specimens decreased, on average, by 14%. It is believed that, first, the weathering induced considerable degradation principally in toughness of the thermoplastic Xenoy matrix, and second, short glass fibres had a good stabilizing effect on the degradation in J_c.

TABLE II Weathering effects on the critical J-integral, J_c, of unreinforced and SGF-reinforced Xenoy specimens

Materials	Notching direction	J_c (kJm^{-2})	
		Unweathered	Weathered for 11 months
Unreinforced Xenoy	L	11.6	9.3
	T	13.0	8.7
SGF31 wt % Xenoy	L	3.6	3.0
	T	5.2	4.5

3.3. Effect of weathering on local ultrasonic velocity

Values of V_R of elastic surface waves were measured for the unreinforced plate as a function of the depth from the weathered surface. They are presented in Fig. 6. The value for the unweathered surface layer was approximately $2.21 \times 10^3\,m\,s^{-1}$. The unweathered specimen exhibited a rather uniform velocity distribution, except for a small portion in the interior where the values were smaller. Weathering for 11 months caused a considerable decrease in V_R up to the depth corresponding to two-thirds of the plate thickness from the weathered surface, giving an average value of $2.13 \times 10^3\,m\,s^{-1}$. On the other hand, a specimen irradiated with ultraviolet rays for 1000 h, showed a slight decrease in V_R for the irradiated surface layer and, contrary to the weathered case, an increase was seen in the interior. Natural weathering should have involved a moisture effect in addition to the effect of degradation by sunlight. Consequently, it may have induced deterioration not only in the surface layer but also in the interior of the plate.

The velocity of Rayleigh waves that travel along the free surface of an elastic half-space, can be expressed as follows [20]

$$V_R = \frac{0.61 + 0.81\nu}{(1+\nu)^{3/2}}(E/\rho)^{1/2} \quad (4)$$

where E is the elastic modulus of the medium, ρ the density, and ν is Poisson's ratio. It is considered that the increase and/or decrease of V_R in Fig. 6 was caused mainly by the change in elastic modulus. This is because only a slight variation was supposed to occur in the density and Poisson's ratio of the material [14]. Thus the natural weathering might have induced some variation in the material's microstructure, which might have reduced E of the surface and core layers. A plausible reason for the increase of V_R in the interior of the ultraviolet-ray irradiated specimen may be some change of the compressive residual stress which could be normally formed in the interior of injection-moulded plate [1]. This scenario might increase the value of E.

3.4. Effect of weathering on microhardness

Fig. 7 presents results of H_u obtained from the surface (skin) and core portions of the unreinforced plate. For the unweathered specimen, the average value of H_u of the core part was smaller than that of the skin layer. This may be reasonable, on considering that the microstructure and residual stresses were differently distributed through the interior during the injection-moulding process [15, 17–19]. Little effect of the natural weathering on H_u was seen. Because the degree of hardness is not exclusively affected by the elastic modulus, but also by the plasticity, H_u was shown to be different from that of Fig. 6 where lower values of V_R were observed for the weathered skin. Irradiation for 1000 h by the artificial ultraviolet rays caused an increase by 26% in H_u of the surface part. It is thought that irradiation by sunlight including ultraviolet rays induced an increase in hardness of the specimen surface, whereas water absorption of the skin layer due to rain and/or moisture contact should have caused a material softening which produced a deterioration of hardness.

3.5. Effect of weathering on fracture surface morphology

Fig. 8 shows scanning electron micrographs taken from the fracture surface of the weathered unreinforced CT specimen. The fracture surface near the initial notch tip was quite flat (see enlarged photograph of area A, in Fig. 8b). In contrast, the fracture surface far from the tip became considerably smaller in thickness due to the large plastic deformation emanating from the surface layer to the interior. Qayyum and White [1] reported that, for PA6.6 and POM, surface microflaws developed caused by the increase of residual

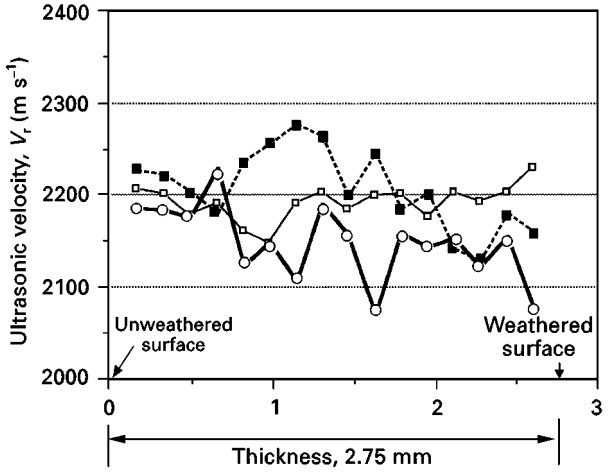

Figure 6 Values of local ultrasonic velocity, V_R, measured through the plate thickness for unreinforced Xenoy plates, which shows significant changes with weathering conditions: (□) unweathered, (○) weathered for 11 months, (■) subjected to UV irradiation for 1000 h.

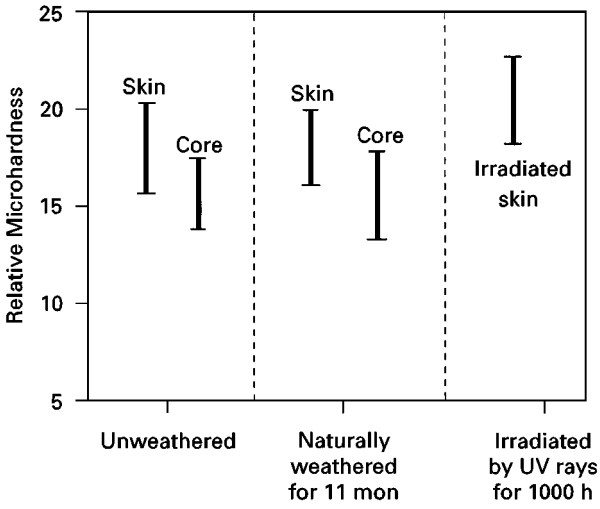

Figure 7 Effects of natural weathering and ultraviolet ray irradation on relative microhardness, H_u, of unreinforced Xenoy plates.

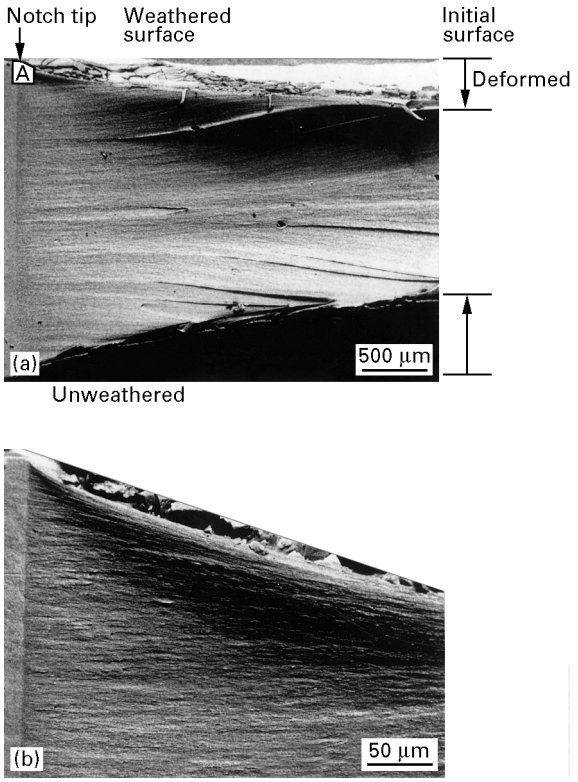

Figure 8 (a) Scanning electron micrograph taken from the fracture surface of an unreinforced CT specimen with an L notch weathered for 11 months. Fracture direction is from left to right. This picture is slightly asymmetric due to tilting during microscopic observation. (b) Enlarged magnification of area A in (a).

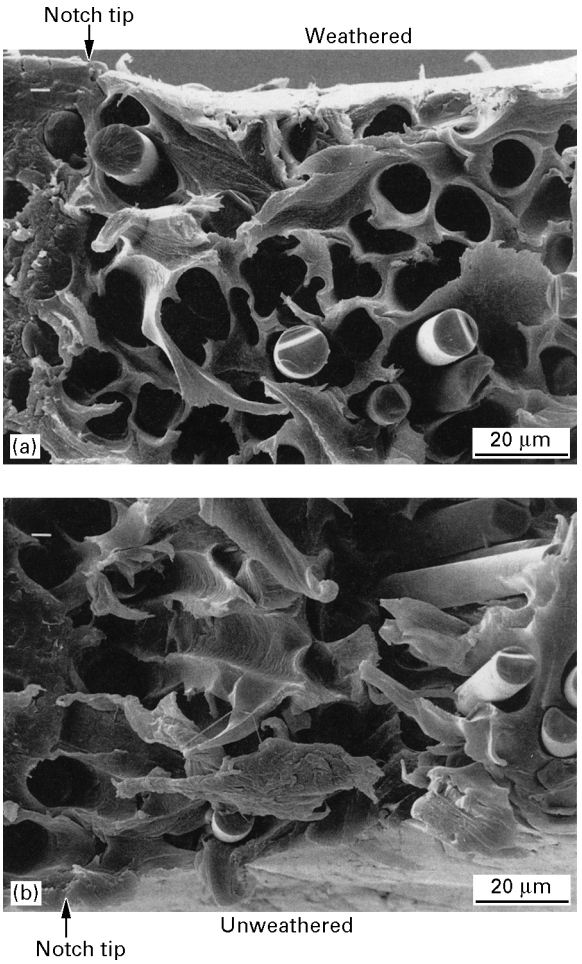

Figure 9 Scanning electron micrographs taken from the fracture surface of an SGF-reinforced CT specimen with an L notch weathered for 11 months. (a) the weathered side, (b) the opposite unweathered side. Fracture direction is from left to right.

tensile stress through weathering which produced multiple surface cracks during tensile testing, i.e. a different failure mechanism, whereas PP did not show much visible surface deterioration on weathering. In this study the fracture pattern of the weathered surface layer, i.e. skin part of the present material showed little difference from that of the opposite unweathered side. Fig. 9 shows scanning electron micrographs taken on fracture surfaces of a weathered SGF 31 %-reinforced CT specimen. Fig. 9a and b are from the skin part and the opposite unweathered skin part, respectively. Changes of the fracture surface due to weathering, i.e. differences in fracture patterns of fibres, matrix and their interfaces, were hardly revealed. It is thought that visible fractures of the present materials were rather insensitive to the weathering effect.

3.6. Sensitivity of material performance to the weathering effects

Polymers are apt to deteriorate in mechanical performance when they are affected by natural weathering [1–10]. Table III summarizes weathering effects of unreinforced and SGF-reinforced Xenoy plates. In respect of global-scale performance, σ_y and fracture surface morphology of the materials were little influenced by weathering for 11 months. However, a significant degradation in J_c was revealed for the unreinforced material. Filling of SGFs exhibited a good anti-degradation effect on J_c, but induced greater degradation in $dJ/d(\Delta a)$ for stable crack propagation due to weathering. On a local scale, a large decrease in V_R was exhibited up to the depth of two-thirds of the plate thickness from the weathered side for the unreinforced plate. However, weathering effects were hardly shown on H_u. On the contrary, an unreinforced plate irradiated for 1000 h with artificial ultraviolet rays exhibited an increase in H_u and a slight deterioration in V_R of the surface layer. It is thus believed, for the present materials, that global-scale performances of J_c and $dJ/d(\Delta a)$ and local scale V_R and H_u were responsive to the weathering conditions.

4. Conclusions

The effects of outdoor and indoor weathering on "Xenoy" plates, without and with short-fibre-reinforcement have been studied by different methods.

1. The weathering induced a large reduction in J_c and a significant decrease in local ultrasonic velocity for unreinforced Xenoy. Although SGF-reinforced Xenoy exhibited an improvement in σ_y and a large reduction in J_c, it revealed some decrease in J_c, but a large degradation in the slope of the R-curve due to the weathering.

TABLE III Summary of weathering effects on unreinforced and SGF-reinforced Xenoy plates

Material performance			Unreinforced Xenoy		SGF-reinforced Xenoy natural weathering
			Natural weathering	Irradiation by UV rays	
Global		σ_y	Little change	–	Little change
		J_c	Large decrease	–	Decrease
		$dJ/d(\Delta a)$	Little change	–	Large decrease
		Fracture morphology	Little change	–	Little change
Local	Skin	V_R	Large decrease	Decrease	–
	Core		Large decrease	Increase	
	Skin	H_u	Little change	Increase	–
	Core		Little change	Little change	

2. However, little weathering effects were shown on yield strength, microhardness and fracture surface patterns.

3. Irradiation for 1000 h by artificial ultraviolet rays caused a considerable increase in microhardness and only a slight deterioration in local ultrasonic velocity of the surface layer of the unreinforced plate.

4. Consequently, it was shown that the measurement of critical *J*-integral and the slope of the *R*-curve in combination with local ultrasonic velocity and microhardness, was an effective way to evaluate the effects of weathering on engineering plastics.

Acknowledgements

The authors thank Y. Hamazaki, Hitacki Kenki Co., who kindly performed the local ultrasonic velocity measurement by scanning acoustic microscopy.

References

1. M. M. QAYYUM and J. R. WHITE, *J. Mater. Sci.* **21** (1986) 2391.
2. H. BERTILSSON, B. FRANZÉN and J. KUBÁT, *Plast. Rubber Process. Appl.* **10** (1988) 137.
3. *Idem*, *ibid.* **10** (1988) 145.
4. M. JUST, *Kunststoffe-German Plastics* **80** (1990) 33.
5. G. KÄMPF, K. SOMMER and E. ZIRNGIEBL, *Prog. Organ. Coatings* **19** (1991) 69.
6. A. SOMMER, E. ZIRNGIEBL, L. KAHL and M. SCHOENFELDER, *ibid.* **19** (1991) 79.
7. M. SEBAA, C. SERVENS and J. POUYET, *J. Appl. Polym. Sci.* **45** (1992) 1049.
8. A. CAMPEOTTO, G. M. FERGUSON and A. JEFFERSON, *Mater. Forum* **16** (1992) 267
9. D. SHIRODA, in "Proceedings of the Endurance Performance of Polymers in Japan", (Japanese Society for Materials Science, Tokyo, 1993) pp. 56–61.
10. T. CZIGÁNY, Z. A. MOHD ISHAK, T. HEITZ and J. KARGER-KOCSIS, *Polym. Composit.* **17** (1996) 900.
11. T. L. ANDERSON, "Fracture Mechanics", 2nd Edn (CRC Press, Ann Arbor, MI, 1995) pp. 131–132.
12. J. D. LANDES and J. A. BEGLEY, "Fract. Analysis" ASTM STP 560 (American Society for Testing and Materials, Philadelphia, PA, 1974) pp. 170–182.
13. S. HASHEMI and J. G. WILLIAMS, *Plast. Rubber Process. Appl.* **6** (1986) 363.
14. K. YAMANAKA, in "Proceedings of the 15th Japan Conference of Materials Science", (Japanese Society for Materials Science, Tokyo, 1992) pp. 59–65.
15. K. FRIEDRICH, L. A. CARLSSON, J. W. GILLESPIE Jr and J. KARGER-KOCSIS, in "Thermoplastic Composite Materials", edited by L.A. Carlsson (Elsevier Science, Amsterdam, 1991) p. 233.
16. N. S. CHOI and K. TAKAHASHI, *J. Mater. Sci.* **31** (1996) 731.
17. A. G. GIBSON and G.A. WILLIAMS, *Polym. Eng. Sci.* **25** (1985) 968.
18. J. A. NAIRN and P. ZOLLER, *J. Mater. Sci.* **20** (1985) 355.
19. T. J. CHAPMAN, J. W. GILLESPIE and J. C. SEFERIS, *J. Compos. Mater.* **24** (1990) 616.
20. J. D. ACHENBACH, "Wave Propagation in Elastic Solids", (North-Holland, Amsterdam, 1975) pp. 187–194.

Received 1 September 1997
and accepted 13 February 1998